Supplementary Information

UV-Driven Self-Repair of Cyclobutane Pyrimidine Dimers in RNA

Sarah J. Crucilla, Dian Ding, Gabriella G. Lozano, Jack W. Szostak, Dimitar D. Sasselov, Corinna L. Kufner

Materials and Methods

Samples

The d(GATT) and d(GA) oligonucleotides were purchased from biomers.net (HPLC purified, lyophilized).

The GAUU, and GA were prepared by solid phase synthesis either on Expedite 8909 or MerMade 6 DNA/RNA synthesizer with phosphonamidites and reagents from ChemGenes (Wilmington, MA) and Glen Research (Sterling, MA). Oligonucleotides prepared in house were deprotected and purified by reverse phase flash chromatography on a 50g C18Aq column using gradient elution over 10 CVs of 0-10% acetonitrile in 20 mM triethylamine bicarbonate (TEAB) buffer (pH 7.5).

The cis-syn CPD lesions[1] were generated by photosensitization of a 1 mM aqueous solution (Supelco, OmniSolv, LS-MS Grade) with 25% volume acetone (Sigma-Aldrich, 270725-2L, ≥ 99.9%) in a fused silica cuvette (Starna Cells, 21-Q-1) at 310 nm (LED, Thorlabs, M310L1) for 60 min (13 mW average power at cuvette position). All RNA samples were degassed with nitrogen for 10 min prior to irradiation. During photosensitization, the sample was mixed continuously. The damaged oligonucleotides were then HPLC purified and lyophilized. For quantum yield determination, the absorbance was kept between OD 0.6 and OD 1.0 (corresponding to several 10nmol of the lyophilized damaged sequences). The oligonucleotides were dissolved in 1.6 mL of 50 mM phosphate buffer (Sigma Aldrich: KH_2PO_4, P5655-100G, ≥ 99.0% and Na_2HPO_4, S7907-100G, ≥ 99.0%) at pH 6.9 (Hach, sensION+ PH3) and then separated to two 800 µL aliquots as reference (dark) and sample (irradiated) which were measured simultaneously in the UV / Vis spectrophotometer. All UV / Vis spectrophotometric measurements were conducted in triplicates.

For ultrafast pump-probe spectroscopy, GA and d(GA) were dissolved in 50 mM deuterated (D_2O) phosphate buffer and kept at concentrations of several millimolar. The absorbance of d(GA) was 1.35 OD and GA 0.86 OD. The time-resolved experiments were performed in a flow cell with 3 mm thick BaF_2 windows and a sample thickness of 100 µm. All measurements were conducted at a room temperature of 24°C under ambient oxygen conditions.

Photometric Setup

The photometric irradiation setup for the determination of the self-repair quantum yields is shown schematically in Figure S1. The 285 nm light of an LED (Thorlabs, M285L5) was projected onto the sample containing UV-fused silica cuvette (Starna Cells, 9B-Q-10-GL14-C, 10 mm path length) by two lenses (Thorlabs, LB4592-UV, f = 60 mm, diameter 2'') and two iris apertures (Thorlabs IDA25). The average power was on the order of 0.3 mW to 0.6 mW and the spot size at the sample position several millimeters. During irradiation, the sample is mixed continuously). The transmitted light was detected by a silicon photodetector (Newport, 918D-UV-OD3R) and a power meter (Newport, 1919-R). Between irradiation intervals, UV-Vis spectra of the sample were recorded by a spectrophotometer (Shimadzu, UV-1900). After 0, 10, 20, and 30 min or irradiation, 5 µL aliquots were taken from the irradiated sample for HPLC analysis.

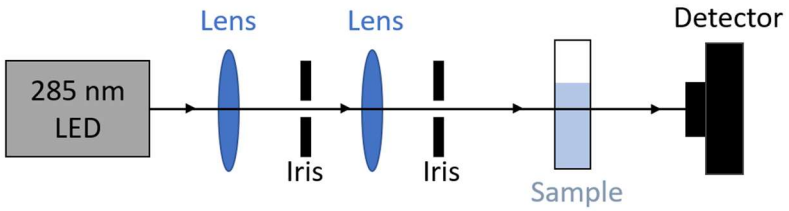

Figure S1. Photometric setup used for the determination of self-repair quantum yields. The 285 nm output of the LED is projected onto the sample cuvette. The transmitted light from the sample is detected by a power sensor.

Data Evaluation

The UV / Vis absorption difference spectra were acquired by subtracting the spectrum of the unirradiated sample from the irradiated samples at different doses. The absorbance at 305 nm was subtracted from all difference spectra. The absorbed dose was determined from the transmitted power, assuming 10% reflection losses. The absorbance difference datapoints at 263 nm for GAU=U and at 266 nm for d(GAT=T) were plotted as a function of the absorbed dose. The slopes were determined by linear fit to the datapoints. The statistical error for each sample was estimated from averaging over triplicate measurements. The systematic error was estimated conservatively to ~40%. The following errors were included in the estimate: 15% for spectrophotometric measurements, 25% for spectral bandwidth of the LED, 20% for sample impurities, 8% for pipetting inaccuracies, 5% for sample positioning inaccuracies during irradiation, 3% for Fresnel reflections, 2% for irradiation time intervals, 1% for beam focusing, and 1% for power detection.

NMR Measurements

^{1}H spectra were acquired at 25 °C on a Varian Oxford AS-400 NMR spectrometer (400 MHz for ^{1}H). Chemical shifts are reported in parts per million (ppm) values on the δ scale. ^{1}H NMR was collected in D_2O and referenced using sodium 2-(trimethylsilyl)-1-propanesulfonate-d6 as internal standard (0 ppm at 25°C). Peaks corresponding to residual TEAB (3.19 and 1.27 ppm) from HPLC purification were observed occasionally. The sample d(GAT=T) and GAU=U was at particular low concentration, so it was dissolved in D_2O and lyophilized for multiple cycles to diminish the presence of water, and then measured by NMR overnight for better resolution.

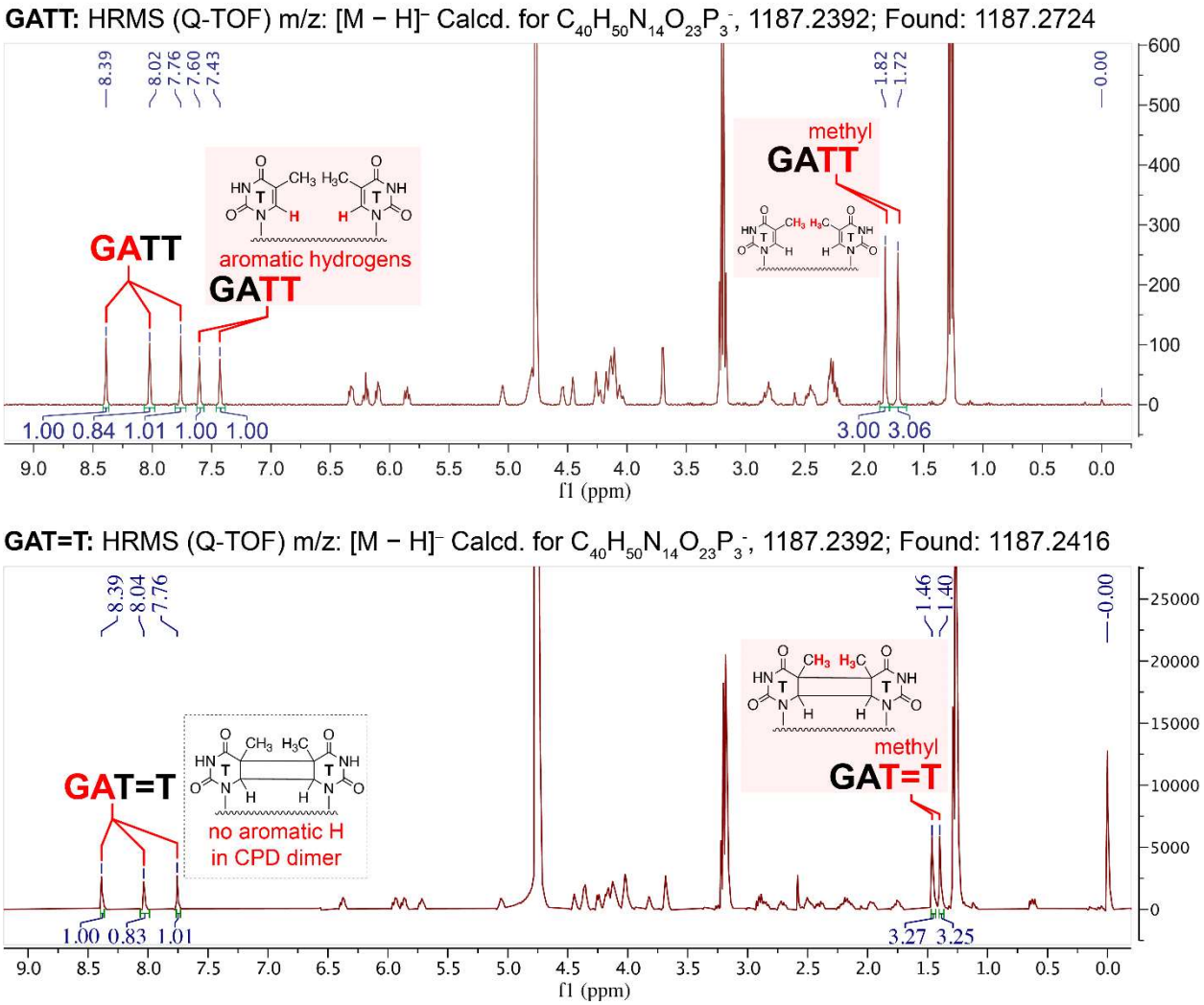

Figure S2. HRMS and NMR spectra of d(GATT) (top) and d(GAT=T) (bottom) in D_2O. The changes in the chemical shifts of the methyl group on thymine from 1.82 & 1.72 ppm to 1.46 & 1.40 ppm indicate the dimer formation, which is in very good agreement with the literature.[2] The thymine aromatic proton peaks of d(GATT) at 7.60 ppm and 7.43 ppm also disappear in the d(GAT=T) spectrum, indicating the dimer formation. The chemical shifts and integrations of the proton peaks on adenine and guanine (7.7–8.4 ppm) are also indicated.

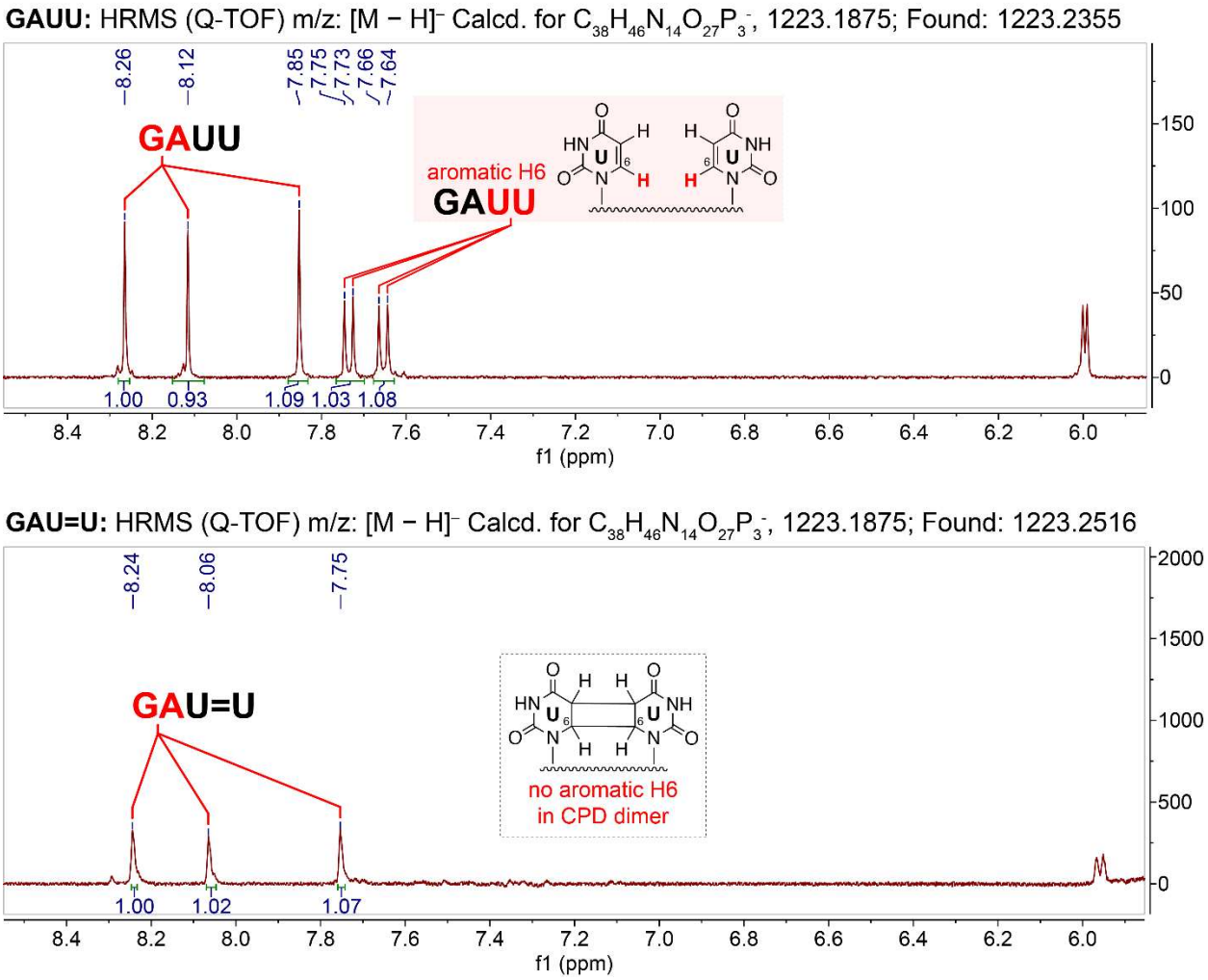

Figure S3. HRMS and NMR spectra of r(GAUU) (top) and r(GAU=U) (bottom) in D_2O. The uridine H6 aromatic proton peaks of r(GAUU) at 7.74 ppm (d, J = 8.1 Hz, 1H) and 7.65 ppm (d, J = 8.1 Hz, 1H) disappear in the GAU=U spectrum, indicating the dimer formation. The chemical shifts and integrations of the proton peaks on adenine and guanine (7.7–8.3 ppm) are also indicated.

Mass Spectrometry

HRMS was carried out on an Agilent 1200 HPLC coupled to an Agilent 6230 TOF mass spectrometer. The sample was separated by IP-RP-HPLC on a 100 mm × 1 mm Xbridge C18 column with 3.5 µm particle size (Water, Milford, MA) with (A) 200 mM 1,1,1,3,3,3-hexafluoro-2- propanol with 1 mM triethylamine, pH 7.0 and (B) methanol. The sample was eluted between 2.5% and 12% B over 16 min with a flow rate of 0.08 mL/min at 30°C. The acquired mass spectra (not shown) confirmed the expected masses of all oligonucleotides studied in this work: GAUU (1224 m/z), GAU=U (1224 m/z), d(GATT) (1188 m/z), and d(GAT=T) (1188 m/z).

HPLC Analysis

The analytical HPLC analysis was performed on a reverse-phase system (Agilent 1100, ZORBAX Eclipse plus C18, 4.6 x 250mm, 5µm, 400 bar). Eluting buffers for the HPLC were buffer A: Acetonitrile (Sigma-Aldrich, 494445-2L) and buffer B: Triethylammonium bicarbonate (Life Technologies Corporation, 90114, 20mM in H_2O). For each run, 5µL of sample was eluted over 37 minutes using a flow of 1 mL/min and a gradient of 5% to 20% of buffer A in buffer B over 12 minutes followed by a 25 minute wash at 25°C.

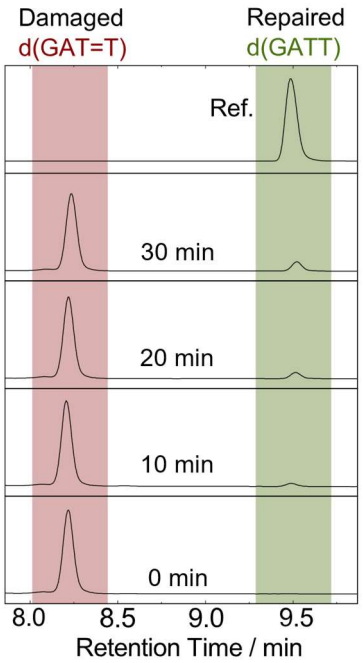

Figure S4. Analytical HPLC analysis of the d(GAT=T) self-repair to d(GATT) at increasing irradiaton times. The top chromatogram shows the intact sequence d(GATT) for reference.

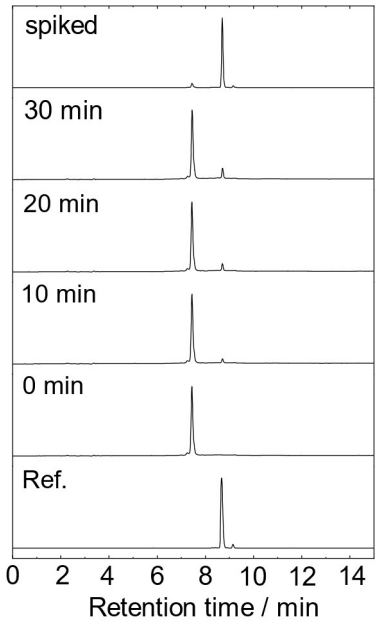

Figure S5. Analytical HPLC analysis of the full 0 min to 15 min range of the GAU=U to GAUU self-repair shown in Figure 2B at increasing irradiaton times. The bottom chromatogram shows the intact sequence GAUU for reference.

Quantum Yield Determination

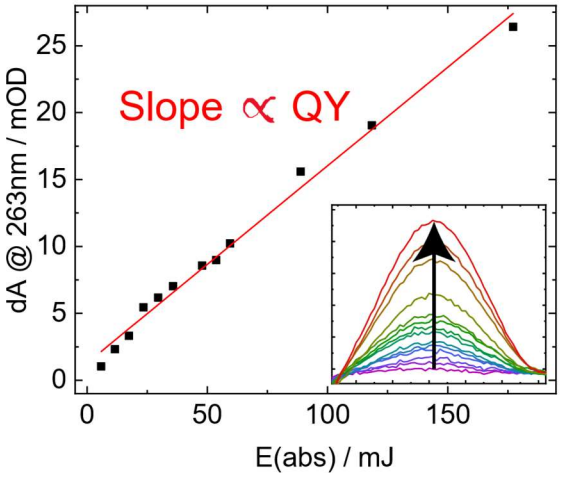

Figure S6. Recovery of the 263 nm absorption band (data points along the black arrow in the absorbance difference spectra, inlet shown here for comparison) upon UV-induced photoreversal of the CPD lesion in the sequence GAU=U as a function of the ab-sorbed dose (black squares). The data can be fitted with a linear trendline (red). The slope of the trendline is linearly proportional to the quantum yield.

The quantum yield, φ, of a photochemical process is defined as the number of molecules of a specific photoproduct, N_{prod}, divided by the number of absorbed photons, N_{abs}.[3]

$$Quantum\ Yield\ \varphi = \frac{N_{prod}}{N_{abs}} \qquad (1)$$

The number of molecules of the photoproduct, here GAUU, can be determined from the absorbance change at 263 nm, $\Delta A|_{263\ nm}$, the molar decadic absorption coefficients of the lesion, $\varepsilon_{U=U}|_{263\ nm}$ and the repaired dinucleotide $\varepsilon_{UU}|_{263\ nm}$, the volume of the sample, V, the Avogadro constant, N_A, and the path length of the cuvette, d.

$$N_{prod} = \frac{\Delta A|_{263\ nm} \cdot V \cdot N_A}{d \cdot [\varepsilon_{UU} - \varepsilon_{U=U}]|_{263\ nm}} \qquad (2)$$

Division of Equation (2) by the absorbed dose, $E_{abs}|_{285\ nm}$, yields:

$$\varphi = \frac{V \cdot N_A \cdot E_{photon}|_{285\ nm}}{d \cdot [\varepsilon_{UU} - \varepsilon_{U=U}]|_{263\ nm}} \cdot \frac{\Delta A|_{263\ nm}}{E_{abs}|_{285\ nm}} \qquad (3)$$

Where $E_{photon}|_{285\ nm}$ is the photon energy at 285 nm. Equation (3) clearly shows the linear proportionality of the quantum yield to the slope of the absorbance difference signal, $\Delta A|_{263\ nm}$, in Figure S6 as a function of the absorbed dose, $E_{abs}|_{285\ nm}$, as all quantities in the first fraction are constants. With a sample volume of 800 µL, a cuvette depth of 10 mm and molar decadic absorption coefficients of $\varepsilon_{UU}|_{263\ nm}$ = 22125 M^{-1} cm^{-1} (determined from scaling to [4]) and $\varepsilon_{U=U}|_{263\ nm}$ = 495 M^{-1} cm^{-1}, we obtain for GAU=U:

$$\varphi \approx 1.55 \cdot 10^{-2} \frac{J}{OD} \cdot \frac{\Delta A|_{263\ nm}[OD]}{E_{abs}|_{285\ nm}[J]} \qquad (4)$$

In case of the d(T=T) lesion, the absorbance change, $\Delta A|_{266\ nm}$, and molar decadic absorption coefficients $\varepsilon_{TT}|_{266\ nm}$ = 18944 M^{-1} cm^{-1} and $\varepsilon_{T=T}|_{266\ nm}$ = 294 M^{-1} cm^{-1} at 266 nm are used,[5] yielding:

$$\varphi \approx 1.80 \cdot 10^{-2} \frac{J}{OD} \cdot \frac{\Delta A|_{266\ nm}[OD]}{E_{abs}|_{285\ nm}[J]} \qquad (5)$$

Sample	Slope / (OD/J)	Quantum Yield / %
d(GAT=T)	0.24 ± 0.06	0.44 ± 0.18
GAU=U	0.15 ± 0.02	0.23 ± 0.09

Table S1. Slopes and Quantum Yields of the Self-Repair (averaged over triplicates).

Photostationary Equilibrium

If irradiated over several hours, the CPD-containing sequences reach an equilibrium between net self-repair and damage formation (into CPD or other unspecified photolesions). The photostationary equilibrium corresponds to the maximum of the plots in Figure S7. The experimental procedure and the corresponding data evaluation as a first order approximation are described in this paragraph. Secondary photoproducts are not considered in this simplified approach.[3]

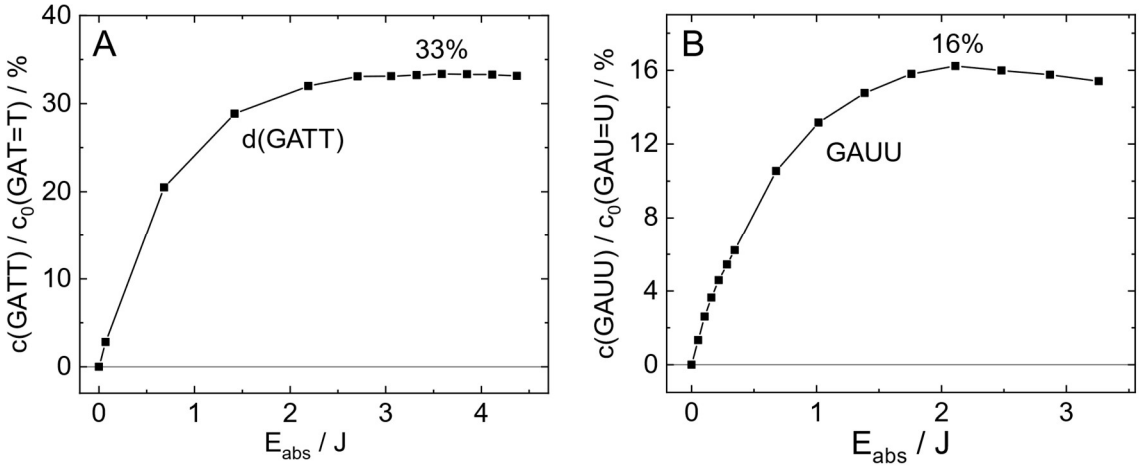

Figure S7. Large-dose irradiations of the samples (A) d(GAT=T) and (B) GAU=U. The photostationary equilibrium of (A) d(GAT=T) to d(GATT) is reached after 33% and (B) GAU=U to GAUU after 16% conversion. The plots show the concentration of the recovered sequence (A) d(GATT) and (B) GAUU divided by the concentration of the starting material (A) d(GAT=T) and (B) GAU=U in percent as a function of the absorbed dose E_{abs}. The experimental starting concentrations were (A) c_0(GAT=T) = 30 µM and (B) c_0(GAU=U) = 21 µM and the irradiation doses P_0 (A) 0.3 mW and (B) 0.6 mW.

The absorbed dose, E_{abs}, (x-axis) was calculated from the irradiation time (t), and the detected power with (P_{trans}) and without (P_0) in the setup shown in Figure S1. Reflection losses are taken into account by scaling factor of 0.9.

$$E_{abs} = (0.9 \cdot P_0 - P_{trans})\, t \qquad (6)$$

The concentration of the starting materials, (A) c_0(GAT=T) and (B) c_0(GAU=U) (y-axis) were calculated from the absorbance of the sample at (A) λ = 266 cm and (B) λ = 263 nm, the cuvette depth (d) and the absorption coefficient of the sample at the respective wavelength following the Beer-Lambert law for homogeneous, non-scattering solutions at low concentration and low light intensities[6], (A):

$$c_0(GAT=T) = \frac{A_0(GAT=T)|_{266nm}}{d \cdot \varepsilon_0(GAT=T)|_{266nm}} \qquad (7)$$

or (B) GAU=U at 263 nm, respectively. The product concentrations, (A) c(GATT) and (B) c(GAUU), (y-axis) were calculated from the measured absorption of the sample, A, after irradiation over t and the absorption coefficients of the damaged, (A) $\varepsilon_{T=T}$ and (B) $\varepsilon_{U=U}$, and undamaged, (A) ε_{TT} and (B) ε_{UU}, sequences, (A):

$$c(GATT) = \frac{A - A_0(GAT=T)|_{266nm}}{d \cdot [\varepsilon_{TT} - \varepsilon_{T=T}]|_{266\,nm}} \qquad (8)$$

or (B) GAU=U at 263 nm, respectively.

Transient Measurements

The basic principles of ultrafast pump-probe spectroscopy can be found in the literature.[7-9] As light source, a Ti:Sa based laser amplifier system (Solstice Ace, Spectra Physics), with an output pulse duration of ~100 fs, 1 kHz repetition rate, 800 nm wavelength was used. The 260 nm excitation pulses were generated in a non-linear amplifier system (Topas Prime + NIRUVis, Light Conversion, Ltd) and stretched to ~1.7 ps by a UV fused silica block (Corning, length 25 cm). The excitation pulses were focused to a pump spot diameter of 120 µm FWHM at the sample position. The excitation energy at the sample position was ~0.96 µJ. The probe pulses were generated in a non-linear amplifier system (Topas Prime + DFG2, Light Conversion, Ltd) and focused to probe spot diameter of ~200 µm FWHM at the sample position inside a transient absorption spectrometer (Helios FIRE, Ultrafast Systems LLC). Pump and probe pulses were spatially overlapped in the sample. The transmitted probe pulses along with a second infrared reference beamline were spectrally dispersed (iHR 320, Horiba) and detected on two 64-channel MCT arrays (MCT-13-2x64, Infrared Associates Inc.). All transient experiments were performed under magic angle conditions. During the measurements, all mid-IR parts of the setup were purged with dry air. The transient lifetimes were determined from a global fitting analysis.[10-12]

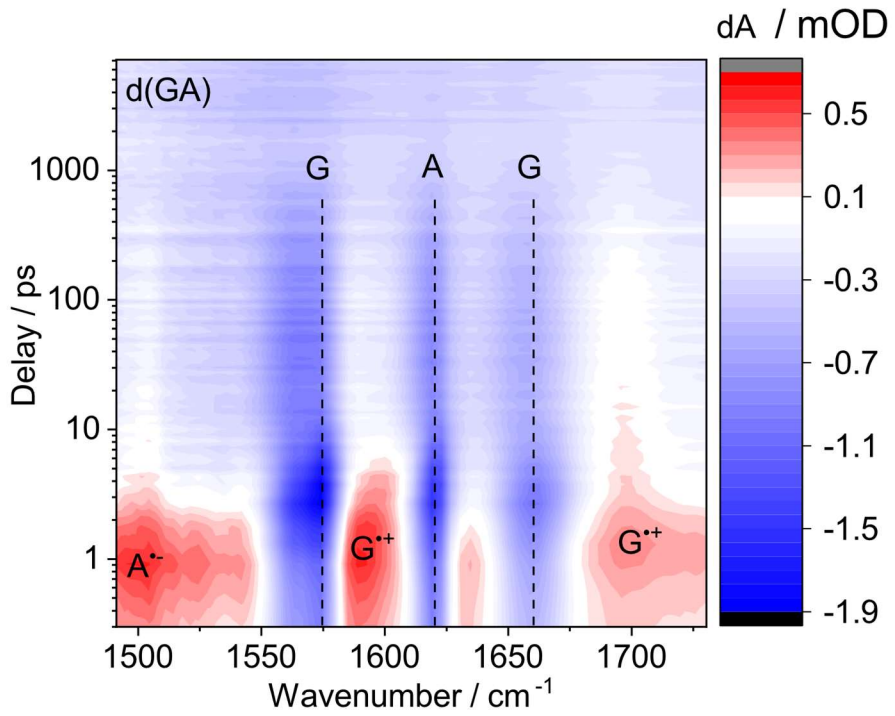

Figure S8. Transient mid-infrared absorption difference spectrum of the DNA dinucleotide d(GA), excited at 260 nm. The negative (blue) ground state bleach bands of G (~1574 cm^{-1} and ~1667 cm^{-1}) and A (1619 cm^{-1}) show excited state lifetimes on the order of 400 ps. Positive bands (red) around 1593 cm^{-1} and 1705 cm^{-1} indicate the presence of the $G^{\bullet+}$ radical cation and a broad signature between 1500 cm^{-1} and 1550 cm^{-1} the $A^{\bullet-}$ radical anion.[13-15]

References

1. M. E. Umlas, W. A. Franklin, G. L. Chan and W. A. Haseltine, *Photochem. Photobiol.*, 1985, **42**, 265-273.
2. T. M. Koning, J. J. van Soest and R. Kaptein, *Eur. J. Biochem.*, 1991, **195**, 29-40.
3. C. L. Kufner, D. B. Bucher and D. D. Sasselov, *ChemSystemsChem*, 2022, e202200019.
4. M. J. Cavaluzzi and P. N. Borer, *Nucleic Acids Res.*, 2004, **32**, e13.
5. Z. Pan, J. Chen, W. J. Schreier, B. Kohler and F. D. Lewis, *J. Phys. Chem. B*, 2011, **116**, 698-704.
6. I. U. o. P. a. A. Chemistry, *Beer–Lambert law (Beer–Lambert–Bouguer law)* 2014.
7. T. Schrader, A. Sieg, F. Koller, W. Schreier, Q. An, W. Zinth and P. Gilch, *Chem. Phys. Lett.*, 2004, **392**, 358-364.
8. K. Haiser, B. P. Fingerhut, K. Heil, A. Glas, T. T. Herzog, B. M. Pilles, W. J. Schreier, W. Zinth, R. de Vivie-Riedle and T. Carell, *Angew. Chem. Int. Ed.*, 2012, **51**, 408-411.
9. W. J. Schreier, J. Kubon, N. Regner, K. Haiser, T. E. Schrader, W. Zinth, P. Clivio and P. Gilch, *J. Am. Chem. Soc.*, 2009, **131**, 5038-5039.
10. H. Satzger and W. Zinth, *Chem. Phys.*, 2003, **295**, 287-295.
11. P. N. Dominguez, M. Himmelstoss, J. Michelmann, F. T. Lehner, A. T. Gardiner, R. J. Cogdell and W. Zinth, *Chem. Phys. Lett.*, 2014, **601**, 103-109.
12. R. Gutierrez-Osuna, H. T. Nagle and S. S. Schiffman, *Sensors Actuators B: Chem.*, 1999, **61**, 170-182.
13. D. B. Bucher, B. M. Pilles, T. Carell and W. Zinth, *Proc. Natl. Acad. Sci. U.S.A.*, 2014, **111**, 4369-4374.
14. D. B. Bucher, C. L. Kufner, A. Schlueter, T. Carell and W. Zinth, *J. Am. Chem. Soc.*, 2016, **138**, 186–190.
15. C. L. Kufner, W. Zinth and D. B. Bucher, *ChemBioChem*, 2020, **21**, 1-6.